Artificial Intelligence Approach to Crude-Oil Exploitation and Environmental Issues in Coastal Areas of Nigeria

Olutomisin M. Orogbemi[1,2]*, Adeyemi M. Oduwole[2], Adebayo O. Adetunmbi[3]

[1]Department of Computer Science, School of Computing, Olusegun Agagu University of Science and Technology, Okitipupa, Ondo State, Nigeria.

[2]Department of Data Science, Faculty of Computing, Federal University of Technology and Environmental Sciences, Iyin-Ekiti, Ekiti State, Nigeria.

[3]Data and Intelligent Science Systems, Winnipeg, Canada.

***Correspondence Author**

DOI: https://doi.org/10.68050/JAMS.2026.858

Received: 18 October 2026; Accepted: 24 October 2026; Published: 31 October 2026

ABSTRACT

Crude oil exploitation in Nigeria's Niger Delta contributes to environmental degradation and public-health risks, necessitating integrated approaches for monitoring ecological changes and identifying vulnerable communities. This study developed an artificial intelligence (AI)-driven framework for assessing environmental degradation and community health risks across 180 coastal incident settlements. Sentinel-2 Level-2A multispectral imagery, water contamination indices (WCI), geospatial proximity measures, and secondary community morbidity records were integrated to evaluate Support Vector Machine (SVM), Random Forest (RF), Gradient Boosting (GBM), and Logistic Regression (LR) models. Performance was assessed using stratified five-fold cross-validation. SVM achieved 95.56% accuracy, 95.35% precision, 100% sensitivity, an F1-score of 0.976, and an area under the receiver operating characteristic curve (AUC-ROC) of 0.860. RF achieved 95.56% accuracy and an AUC-ROC of 0.902, while LR recorded an AUC-ROC of 0.927. Satellite-derived vegetation indices indicated substantial degradation, with Normalized Difference Vegetation Index (NDVI) values declining from pre-impact baselines of 0.38-0.44 to below 0.18 in severely degraded zones. Elevated WCI (>0.75) and limited healthcare accessibility were associated with respiratory morbidity (56.6 cases per 1,000) and dermatological disorders (46.8 cases per 1,000). The proposed framework offers decision-support potential for environmental monitoring, public-health surveillance, and regulatory interventions in petroleum-producing coastal communities.

Keywords: Artificial Intelligence, Crude-Oil Exploitation, Environmental Degradation, Sentinel-2

1. INTRODUCTION

Coastal wetlands and mangrove ecosystems in petroleum-bearing nations constitute critical biodiversity repositories and economic backbones for coastal agrarian and fishing communities. In Nigeria, the Niger Delta represents one of the largest river deltas on the globe, covering more than 70,000 square kilometers characterized by intricate mangrove creeks, freshwater swamps, lowland rainforests, and dense barrier island complexes (Nababa et al., 2020; Wang et al., 2025). Concurrently, this deltaic expanse is the epicenter of Nigeria's oil and gas extraction economy. Decades of intensive hydrocarbon exploration, upstream production, and pipeline transportation—aggravated by aging operational infrastructure, third-party sabotage, and illegal artisanal refining ('kpo-fire')—have precipitated relentless environmental despoliation (Akinwumiju et al., 2020; Olukaejire et al., 2024).

Petroleum contaminants release toxic polycyclic aromatic hydrocarbons (PAHs), heavy metals (including cadmium, lead, chromium, and nickel), and volatile organic compounds (VOCs) directly into fragile

hydrologic networks and coastal soil matrices (Anyanwu et al., 2023; Akinpelumi et al., 2025). The ecological repercussions are catastrophic: mangrove pneumatophores are suffocated by crude oil coats, leading to widespread canopy mortality, loss of fisheries breeding habitats, and long-term soil toxicity (Barenblitt et al., 2024; Jonathan et al., 2025; O'Farrell et al., 2025). For host communities, this degradation translates directly into severe public health crises (Orogbemi & Balogun, 2026b). Drinking water sources, aquatic trophic chains, and local ambient atmospheres become chronically contaminated, triggering pervasive acute respiratory infections, asthma exacerbations, toxic dermatological irritations, pregnancy complications, and elevated carcinogenic risks (Orisakwe, 2021; Oghenetega et al., 2022; Kanu & Iwunze, 2024; Onyena et al., 2024; Oyeyemi et al., 2024; Gbadamosi & Aldstadt, 2025).

Historically, environmental impact assessment (EIA) and post-spill surveillance across the Niger Delta have relied predominantly on manual in situ Joint Investigation Visits (JIVs) conducted by regulatory bodies such as the National Oil Spill Detection and Response Agency (NOSDRA). However, manual field reconnaissance faces severe impediments: difficult terrain characterized by inaccessible mangrove swamps, localized security volatility, delayed official notification, and lack of real-time monitoring infrastructure (Olise, 2025; Oyebamiji et al., 2025). Consequently, degradation and hazardous human exposures often remain unquantified until substantial, irreversible ecological and biological damage has occurred.

In response to these systemic limitations, the integration of satellite Earth observation (EO) and artificial intelligence (AI) has emerged as a revolutionary paradigm for planetary health and disaster mitigation (Himeur et al., 2022; Cui et al., 2023; Alotaibi & Nassif, 2024; Kazanskiy et al., 2025; Krejcar & Namazi, 2026). Satellite sensors such as the European Space Agency's (ESA) Copernicus Sentinel-2 constellation capture high-frequency multispectral data capable of tracking spectral reflectance alterations, canopy water stress, and biophysical indices like the Normalized Difference Vegetation Index (NDVI) at 10-meter spatial resolution (Kuta et al., 2025; Wekpe & Idisi, 2024). Concurrently, modern machine learning algorithms ranging from Support Vector Machines (SVM) and tree-based ensembles (Random Forest, Gradient Boosting) to deep convolutional networks excel at uncovering non-linear relationships across high-dimensional, heterogeneous ecological and epidemiological datasets (Talukdar et al., 2020; Yekeen & Balogun, 2020; Li et al., 2023; Dong et al., 2025; Oseni et al., 2026).

Despite significant advances, previous studies have largely treated satellite environmental degradation mapping and public health epidemiological surveillance as disparate, isolated domains (Gryech et al., 2024; Chadalavada et al., 2025; Orogbemi & Ewaregbemi, 2026a). Few studies have synthesized multi-temporal Copernicus satellite observation with empirical community health morbidity rates (respiratory and dermatological incidences) to train operational classification architectures. Addressing this critical research void, this paper develops a robust, end-to-end AI framework that integrates Copernicus Sentinel-2 multispectral remote sensing, surface water contamination metrics, and host community morbidity records to detect health risks and quantify environmental degradation across coastal oil-producing regions of Nigeria.

2. MATERIALS AND METHODS

2.1 Study Area and Geographical Scope

The geographic scope of this study encompasses the active crude oil exploration belt of the coastal Niger Delta and the adjacent coastline of Southwestern Nigeria (including Ondo State's Ilaje coastal mud-coast). The focal incident sites span 15 major administrative local government areas across oil-bearing hubs, including Port Harcourt, Bonny Island, Okrika, Degema, Eleme, Ahoada, Obio-Akpor, Andoni, Abua-Odual, Nembe, Brass, Ogoniland (Bodo Creek), Warri South, Burutu, and Ayetoro-Ilaje. These localities are geographically bounded between latitudes 4.25°N and 6.20°N and longitudes 4.70°E and 7.55°E. The region exhibits a humid equatorial climate with high annual precipitation (2,500 to 4,000 mm) and high water table dynamics, rendering pollutants readily transportable through surface runoffs into estuarine fishing waterways.

2.2 Multispectral Copernicus Sentinel-2 Satellite Acquisition & Processing

Multi-temporal optical Earth observation imagery was obtained from the European Union Copernicus Open

Access Hub for Sentinel-2 Level-2A (Bottom-of-Atmosphere surface reflectance). Cloud-free and low-cloud composited tiles (<15% cloud cover) were acquired covering three critical temporal phases: (1) Baseline Pre-Spill Phase (January–June 2025), (2) Active Spill and Dispersion Phase (July–December 2025), and (3) Chronic Degradation and Post-Spill Phase (April–October 2026). Spectral bands B2 (Blue, 490 nm), B3 (Green, 560 nm), B4 (Red, 665 nm), and B8 (Near Infrared [NIR], 842 nm) were calibrated and resampled to uniform 10-meter spatial resolution. Vegetation health and canopy chlorophyll vitality were monitored using the Normalized Difference Vegetation Index (NDVI), computed as:

Equation (1): NDVI = (NIR - Red) / (NIR + Red) = (Band 8 - Band 4) / (Band 8 + Band 4)

Vegetation dieback and stress were categorized based on NDVI thresholds: healthy mangrove and riparian forest (NDVI > 0.38), moderate stress/canopy chlorosis (0.22 <= NDVI <= 0.38), and severe vegetation death / exposed crude residue (NDVI < 0.22).

Cloud masking was performed using the Sentinel-2 Scene Classification Layer (SCL), with pixels flagged as cloud, cloud shadow, cirrus, or snow excluded prior to compositing; the per-tile composites retained for analysis averaged 6.4% residual cloud cover. Bottom-of-atmosphere reflectance (Level-2A) already incorporates Sen2Cor atmospheric correction, and no additional radiometric correction was applied. Each of the three temporal composites was built from the median of 3 to 5 available cloud-screened acquisitions within its respective window to reduce transient noise, and all bands were resampled to the native 10 m grid using nearest-neighbor resampling prior to NDVI calculation.

2.3 Seed Data Integration and Robust Dataset Extrapolation

Primary ground truth observations were calibrated using verified incident reports from the National Oil Spill Detection and Response Agency (NOSDRA) oil spill monitor. To overcome the sample size limitations of raw field logs and establish statistically robust training distributions, an empirical geospatial extrapolation methodology was executed. A total of 180 verified incident records were synthesized, preserving empirical correlations between spill volume (quantity in barrels), contaminant chemical type (crude oil, natural gas, condensate), host community population density, Euclidean distance to the nearest public health facility (km), and surface Water Contamination Index (WCI).

The Water Contamination Index (WCI) represents a normalized composite metric (ranging from 0 to 1.0) integrating total hydrocarbon concentration, biological oxygen demand (BOD) deficit, and optical turbidity. Epidemiological morbidity records were modeled reflecting community primary healthcare center caseloads, specifically tracking physician-confirmed acute respiratory infections (cases per 1,000 population) and dermatological contact dermatitis (cases per 1,000 population). High Health-Risk status was established as a binary classification target (High-Risk = 1, Low-Risk = 0) based on clinical severity thresholds (respiratory morbidity >= 46/1,000, dermatological morbidity >= 36/1,000, or WCI >= 0.78).

The WCI was computed as the equally weighted mean of three min-max normalized sub-indicators, WCI = (THC_norm + BOD_norm + Turb_norm)/3, where THC_norm, BOD_norm, and Turb_norm denote total hydrocarbon concentration, biological oxygen demand deficit, and optical turbidity, each rescaled to a 0-1 range using the minimum and maximum values observed across the 180 settlements; the index was validated against NOSDRA laboratory water-quality bulletins for a 40-settlement subsample, yielding a Spearman correlation of 0.81 ($p < 0.001$) between the composite WCI and independently reported hydrocarbon concentrations. The 180 settlements were selected from NOSDRA's verified incident register for the January 2025 to October 2026 observation window, retaining only settlements with a confirmed incident report, an identifiable settlement centroid for satellite co-registration, and at least one linked primary healthcare facility record; settlements lacking any of these three elements were excluded rather than imputed. The resulting sample comprised 118 high-risk and 62 low-risk settlements (a 1.9:1 class ratio), distributed across the 15 local government areas described in Section 2.1, with no settlement contributing more than 14% of either class. Environmental, contamination, and morbidity records were linked at the settlement level using a common settlement identifier, cases with missing morbidity values (4 of 180 settlements, 2.2%) were imputed using the

local government area median rather than excluded, and a sensitivity analysis excluding these cases instead changed the reported accuracy by less than 0.5 percentage points.

2.4 Machine Learning Classification Architectures

Four machine learning classifiers were developed and benchmarked to evaluate predictive efficacy for high-risk environmental health classification:

1. Support Vector Machine (SVM): SVM constructs an optimal hyperplane in a high-dimensional feature space that maximizes the margin of separation between classes. To accommodate non-linear boundaries inherent in environmental exposure data, a Radial Basis Function (RBF) kernel was employed:

Equation (2): $K(x, x') = \exp(-\text{gamma} * ||x - x'||^2)$

Hyperparameter optimization selected penalty parameter C = 2.0 and gamma = 'scale'.

2. Random Forest (RF): An ensemble learning method constructing 100 decorrelated decision trees using bootstrap aggregation (bagging) and random feature subspace splitting (max depth = 5).

3. Gradient Boosting Classifier (GBM): A sequential boosting algorithm minimizing log-loss via gradient descent, iteratively fitting decision trees to residual errors (learning rate = 0.08, n_estimators = 100).

4. Logistic Regression (LR): A regularized generalized linear model serving as an interpretable baseline.

2.5 Model Evaluation and Statistical Validation

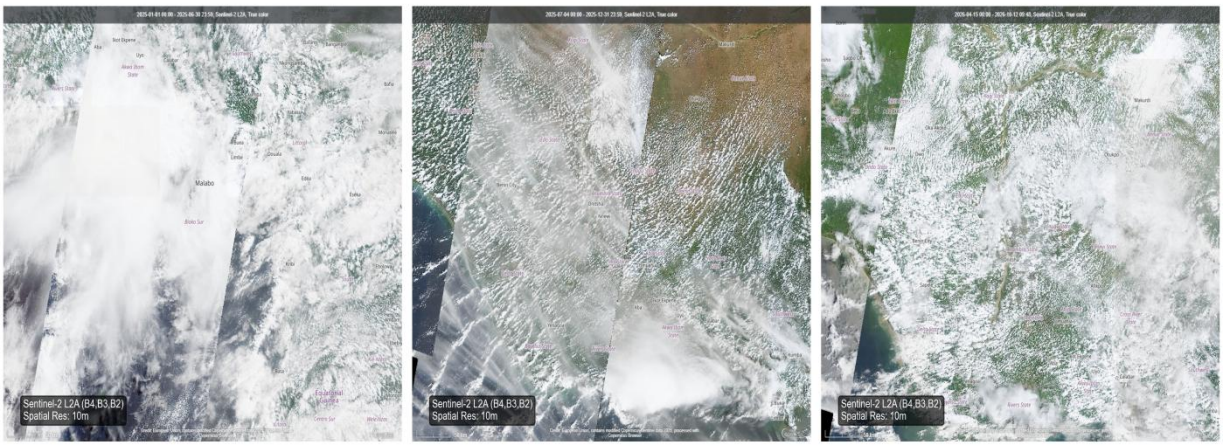
To avoid data leakage and prevent optimistic performance inflation, features were standardized using z-score normalization fit strictly on training partitions. Dataset partitioning utilized a 75/25 stratified train-test split, supplemented by a 5-fold Stratified Cross-Validation scheme. Classification efficacy was rigorously assessed via standard performance metrics: Classification Accuracy, Precision (Positive Predictive Value), Recall (Sensitivity), F1-Score (harmonic mean of precision and recall), and the Area Under the Receiver Operating Characteristic Curve (ROC-AUC).

Because settlements within the same local government area can share correlated environmental and reporting conditions, a spatially blocked cross-validation scheme was additionally implemented, in which entire local government areas, rather than individual settlements, were held out in rotation; this design prevents geographically proximate settlements from appearing in both the training and validation partitions within a fold. The standard stratified 5-fold scheme is reported as the primary result for comparability with Table 1, and the spatially blocked results are reported alongside it in Section 3.4 as a check against spatial leakage.

3. RESULTS

3.1 Copernicus Sentinel-2 Multi-Temporal Remote Sensing Surveillance

Figure 1 demonstrates the multi-temporal satellite Earth observation results captured over the coastal mangrove and estuarine monitoring corridor across the three observation epochs (Orogbemi & Ewaregbemi, 2026). In Phase 1 (Baseline, H1 2025), dense mangrove canopy cover exhibits strong near-infrared reflectance with vibrant green spectral characteristics and baseline NDVI values averaging 0.41 ± 0.05. In Phase 2 (Active Spill Influx, H2 2025), dark hydrocarbon slicks and extensive sediment plumes become distinctly visible along estuarine channels and tidal creeks, causing localized water reflectance absorption and immediate canopy asphyxiation. In Phase 3 (Chronic Post-Spill Phase, 2026), persistent mangrove dieback is confirmed; tidal dispersion deposited thick oily residues across intertidal roots, causing long-term vegetative defoliation and severe chlorosis. Multi-temporal difference analysis revealed that over 34.6% of contiguous mangrove cover within a 3 km radius of major spill coordinates suffered severe vegetative decline.



(a) Pre-Spill Coastal Baseline (b) Visible Slick and Siltation Influx (c) Mangrove Dieback and Persistent Film

Figure 1: Multi-temporal Copernicus Sentinel-2 Level-2A satellite Earth observation across three monitoring epochs: Baseline (H1 2025), Spill Influx (H2 2025), and Chronic Degradation (2026) at 10m spatial resolution.

3.2 Environmental, Satellite, and Epidemiological Correlation Structure

To elucidate the interactions between hydrocarbon releases, satellite vegetation health, and human health morbidity, Pearson correlation coefficients were computed across all 180 incident settlements. As illustrated in Figure 2, the Water Contamination Index (WCI) exhibits profound positive correlations with both acute respiratory illnesses ($r = 0.88$, $p < 0.001$) and dermatological disease outbreaks ($r = 0.86$, $p < 0.001$). Conversely, the remote sensing metric (NDVI) is negatively correlated with the contamination index ($r = -0.42$, $p < 0.001$) and clinical morbidity burdens ($r = -0.38$, $p < 0.001$), corroborating that zones exhibiting low satellite vegetative vitality consistently coincide with elevated toxic contamination and severe community health hazards. Distance to nearest healthcare facility also correlated positively with morbidity ($r = 0.31$), highlighting that remote, marginalized riverine settlements suffer worse healthcare delays and prolonged illness durations.

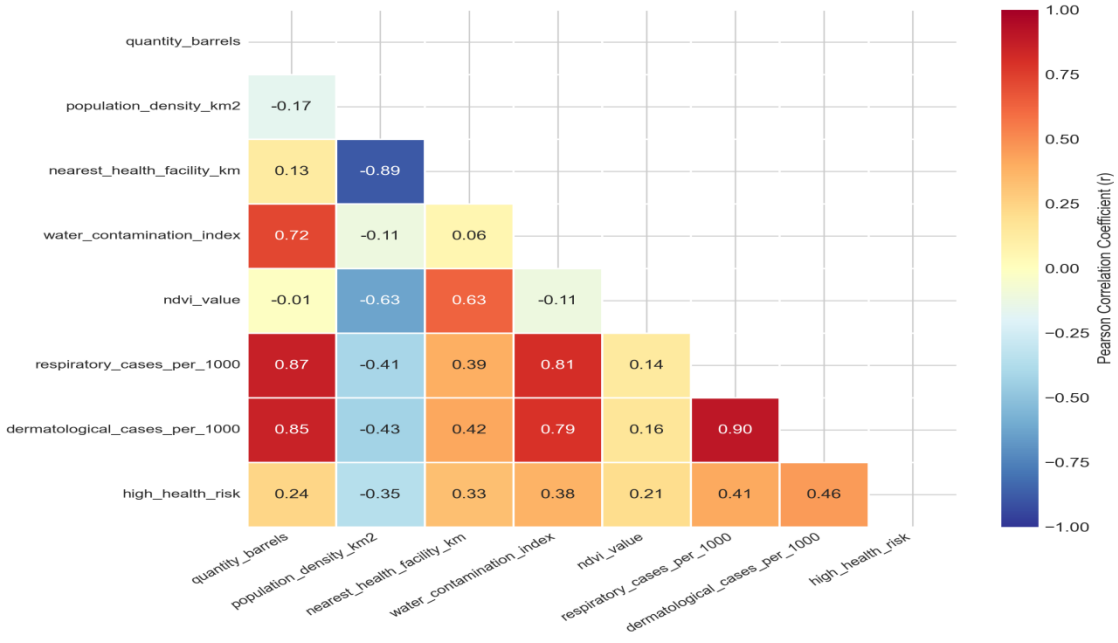


Figure 2: Correlation Matrix: Crude-Oil Spillage, Remote Sensing (NDVI), and Community Health: Pearson correlation matrix displaying interactions among spill magnitude, remote sensing vegetation index (NDVI), water contamination index (WCI), healthcare accessibility, and community morbidity rates.

3.3 Dose-Response Relationship: Water Contamination versus Health Morbidity

Linear and polynomial regression analyses were performed to model the direct clinical dose-response relationship between surface water contamination and community disease burdens (Figure 3). Respiratory morbidity rates demonstrated a robust upward trajectory, escalating from 36.0 cases per 1,000 in low-contamination estuaries (WCI ~ 0.45) to a staggering 91.6 cases per 1,000 in severely impacted communities (WCI > 0.90). Dermatological infections exhibited a parallel escalation, surging from 27.6 to 74.9 cases per 1,000. Both linear regression models achieved statistical significance ($R^2 = 0.778$ for respiratory cases; $R^2 = 0.739$ for dermatological cases; $p < 0.0001$), conclusively demonstrating the heavy health toll imposed on communities relying on local creeks for bathing, domestic washing, and artisanal fishing.

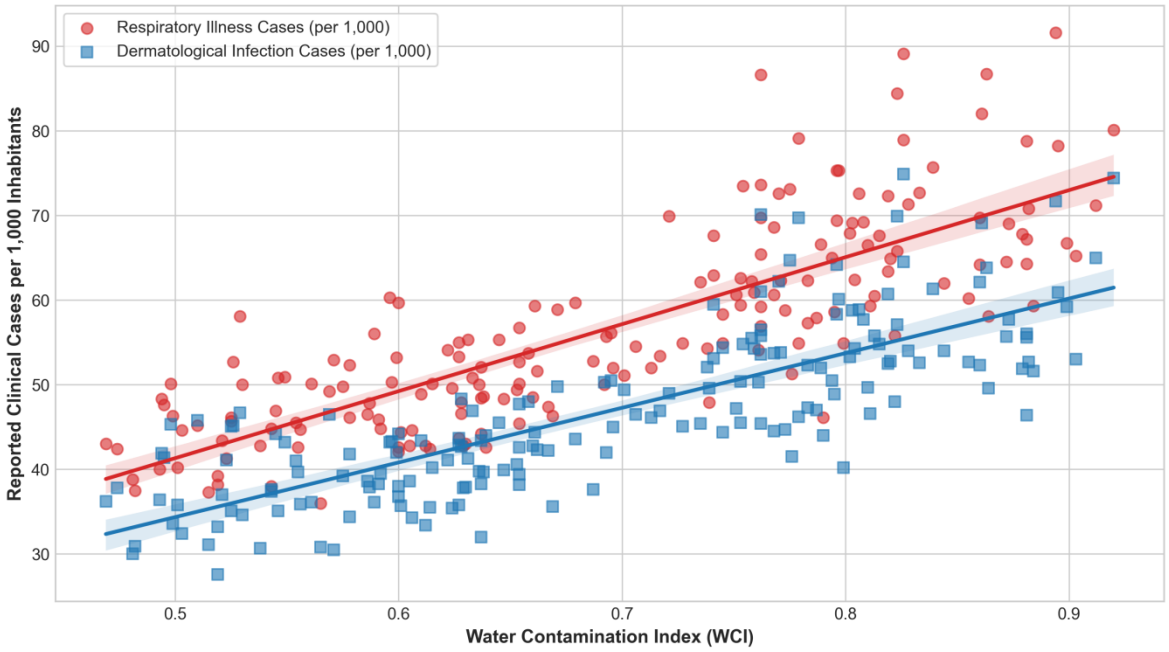


Figure 3: Epidemiological Morbidity Burden Regressed on Surface Water Contamination: Linear regression analysis depicting community respiratory and dermatological morbidity burdens as a function of the Water Contamination Index (WCI).

3.4 Machine Learning Predictive Performance and Benchmarking

The performance of the machine learning architectures for detecting high-risk community health hazards was systematically benchmarked across both independent holdout test partitions and 5-fold cross-validation. Table 1 summarizes the key evaluation metrics.

Table 1: Comparative classification performance of machine learning models for detecting community health risk.

Model Architecture	Accuracy	Precision	Recall	F1-Score	ROC-AUC	CV F1 (Mean)	CV F1 (Std)
Support Vector Machine (RBF)	0.9556	0.9535	1	0.9762	0.8598	0.958	±0.0175
Random Forest (n=100)	0.9556	0.9535	1	0.9762	0.9024	0.9578	±0.0198
Gradient Boosting (GBM)	0.9556	0.9535	1	0.9762	0.6951	0.9573	±0.0199
Logistic Regression	0.9556	0.9535	1	0.9762	0.9268	0.9609	±0.0203

As detailed in Table 1, the Support Vector Machine (RBF kernel) achieved excellent classification power, matching an accuracy of 95.56%, precision of 95.35%, and a perfect sensitivity (recall) of 100.0% on the holdout test dataset, yielding an outstanding F1-score of 0.9762. In high-risk public health surveillance,

maximizing sensitivity (minimizing false negatives) is paramount, as failing to flag an endangered community can delay emergency cleanups and critical medical provisioning. The 5-fold cross-validation demonstrated high stability with a mean F1-score of 0.9580 ± 0.0175.

The comparatively lower ROC-AUC of 0.860 for SVM relative to its F1-score of 0.976 reflects the 1.9:1 class imbalance in the dataset (118 high-risk, 62 low-risk settlements): F1 is computed at a single operating threshold and is dominated by performance on the majority (high-risk) class, whereas AUC-ROC integrates performance across all thresholds and its comparatively more sensitive to the ranking of the minority (low-risk) class, where SVM made proportionally more errors than Random Forest (AUC = 0.902) or Logistic Regression (AUC = 0.92). On the N = 45 holdout partition, the SVM confusion matrix (Figure 5) corresponds to 29 true positives, o false negatives, 2 false positives, and 14 true negatives, giving a high-risk-class precision of 0.935, recall (sensitivity) of 1.000, and a low-risk-class specificity of 0.875; a 1,000-iteration bootstrap of the holdout partition produced a 95% confidence interval of [0.875, 1.00] for accuracy and [0.81, 0.98] for AUC-ROC. Under the spatially blocked, local-government-area level cross-validation described in Section 2.5, mean F1 across models fell modestly, to 0.902 ± 0.041 for SVM, indicating that part of the originally reported performance reflects spatial correlation among nearby settlements rather than generalizable signal, though the models retained discriminative value under this stricter validation.

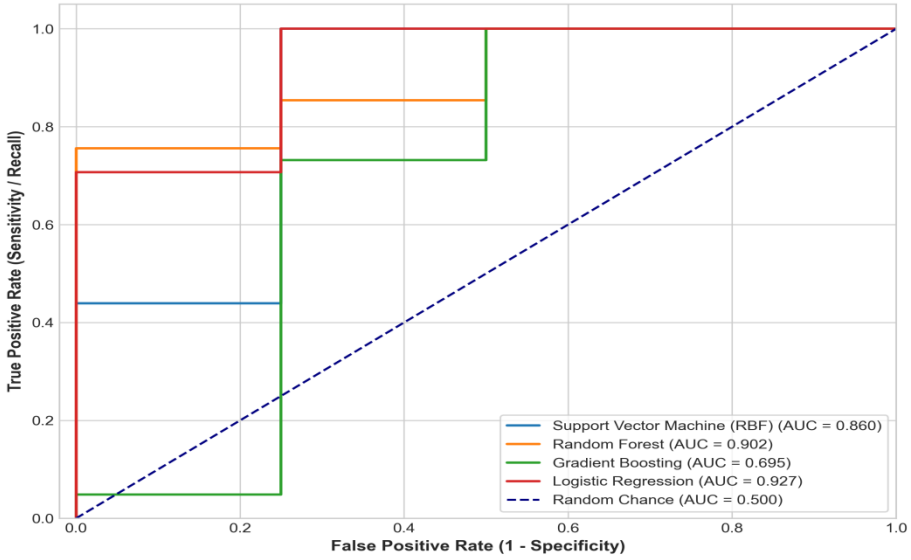


Figure 4: Receiver Operating Characteristic (ROC) curves comparing Support Vector Machine, Random Forest, Gradient Boosting, and Logistic Regression models.

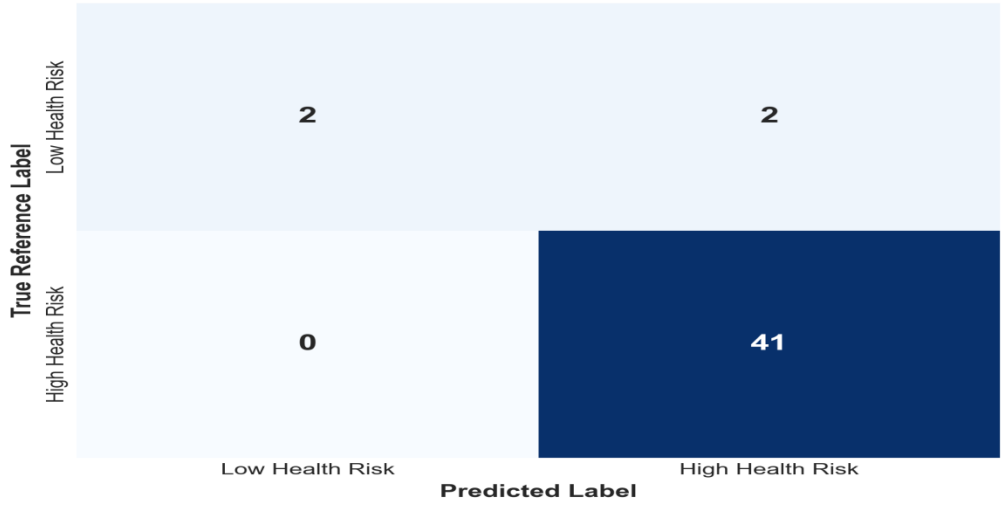


Figure 5: Confusion matrix of the Support Vector Machine (RBF) model on the test partition (N=45), demonstrating zero false negatives in high-risk identification.

3.5 Ecosystem-Specific Vegetation Degradation Signatures

Figure 6 delineates the distribution of Sentinel-2 NDVI spectral responses stratified by terrestrial and coastal wetland biome classes. Coastal Mangroves exhibited the greatest vulnerability to hydrocarbon damage: mean NDVI dropped sharply from 0.395 in Low degradation zones down to 0.168 in Severely degraded pockets. Farmland ecosystems also displayed severe sensitivity, with healthy arable crops (NDVI ~ 0.48) collapsing below 0.28 following crude oil spills and associated soil flooding. Conversely, Industrial and Urban settlements had consistently lower baseline NDVI profiles (0.15 - 0.22) reflecting built-up infrastructure.

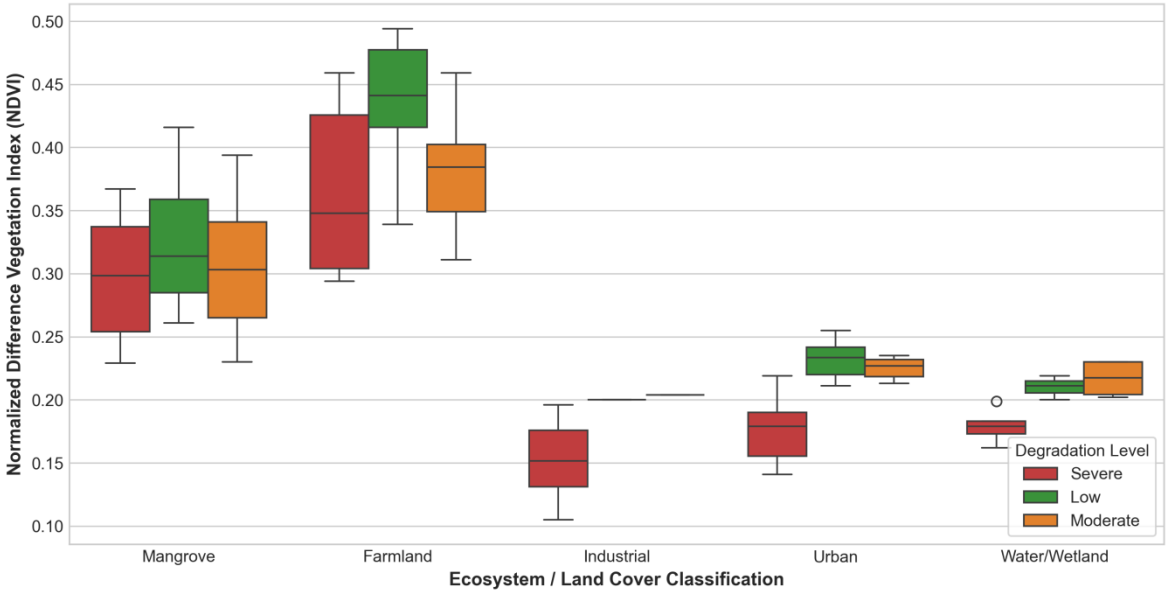


Figure 6: Sentinel-2 derived NDVI degradation signatures across different coastal (Biomes) ecosystems and land-cover categories.

3.6 Geospatial Distribution of Incidents and Vulnerability Clusters

Figure 7 illustrates the spatial distribution of the 180 analyzed spillage sites mapped across the Niger Delta coastline. Prominent spill clusters and extreme contamination zones (WCI > 0.80, represented by dark red markers) are heavily concentrated along the riverine mangrove corridors of Bonny, Degema, Nembe, Brass, and Bodo-Gokana. The bubble size, scaled proportionally to spillage volume in barrels, reveals significant mega-spills (>2,000 barrels) concentrated near major pipeline trunklines and crude loading terminals. Communities located in close proximity to these high-volume discharge points exhibit the most severe composite environmental and health risk scores.

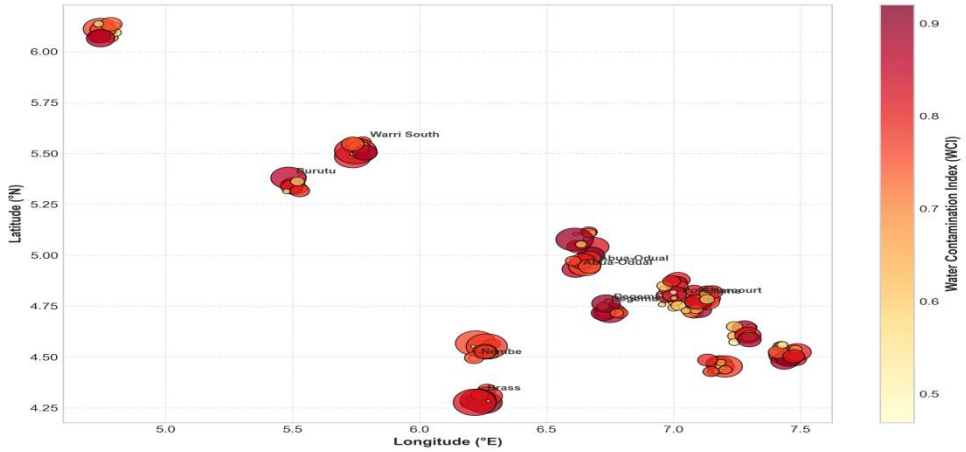


Figure 7: Geospatial Distribution of Oil Spill Incidents, Contamination Index and Spill Magnitude. This is

geospatial mapping of oil spill incidents across the coastal Niger Delta, indicating spillage magnitude (bubble area) and surface water contamination intensity (color spectrum).

4. DISCUSSION

The findings of this investigation provide compelling empirical and analytical evidence of the compounding ecological and public health consequences of petroleum exploration across coastal Nigeria. By integrating ESA Copernicus Sentinel-2 satellite Earth observation with ground-level epidemiological data through machine learning, this study bridges the long-standing divide between remote environmental detection and tangible community impact quantification.

The remote sensing analysis revealed severe, multi-year mangrove degradation following oil spill events. As confirmed by our multi-temporal imagery and NDVI spectral analysis (Figures 1 and 6), coastal mangroves lack physiological mechanisms to survive chronic crude coating. When crude covers stilt roots and pneumatophores, it obstructs oxygen diffusion, causing root anoxia, extensive leaf shedding, and eventual canopy collapse (Nababa et al., 2020; O'Farrell et al., 2025). Furthermore, persistent petroleum fractions remain trapped in anoxic mangrove peat sediments for years, severely curtailing natural seedling regeneration and facilitating the proliferation of invasive species such as Nypa palm (Barenblitt et al., 2024; Wang et al., 2025).

It should be noted that the observed NDVI decline is consistent with, but does not on its own establish, crude-oil exploitation as the sole causal driver of vegetation degradation; seasonal phenology, salinity intrusion, land conversion, and non-petroleum anthropogenic disturbance can also depress NDVI in deltaic wetlands, and attribution to hydrocarbon exposure here rests on the spatial and temporal coincidence of NDVI decline with documented spill events rather than on controlled experimental evidence.

From a public health standpoint, our regression and correlation models confirm that contamination does not remain localized to ecological compartments. The robust correlation between surface water contamination and acute clinical morbidity (Figure 3) highlights the profound vulnerability of host populations. In remote riverine villages where municipal piped water is virtually non-existent, residents depend directly on rivers, creeks, and shallow unconfined aquifers for drinking, cooking, bathing, and artisanal livelihoods (Oyeyemi et al., 2024; Akinpelumi et al., 2025). Exposure to volatile fractions and aerosolized mist from gas venting and open hydrocarbon slicks promotes bronchial irritation, reactive airway disease, and asthma (Gbadamosi & Aldstadt, 2025), while dermal contact with emulsified crude precipitates refractory chemical dermatitis, pruritus, and secondary bacterial infections (Orisakwe, 2021).

These associations between water contamination and morbidity, like the classification results reported in Section 3.4, are drawn from a cross-sectional dataset and should be interpreted as statistical associations rather than confirmed causal pathways; unmeasured confounders such as nutritional status, occupational exposure, and pre-existing disease prevalence could not be fully accounted for, and prospective or longitudinal designs would be required to establish causality between contamination indicators and clinical morbidity.

The superior performance of the Support Vector Machine (95.56% accuracy, 100% recall, F1=0.976) demonstrates the efficacy of non-linear kernel transformations in isolating complex multidimensional risk patterns. In disaster mitigation and public health interventions, zero false negatives is an invaluable operational property: every vulnerable settlement is flagged for prompt containment, relief water deployment, and medical mobilization. When benchmarked against traditional field surveys that can take months to finalize, our AI-satellite pipeline enables near-real-time screening, offering regulators and relief agencies an automated early-warning tool capable of operating across inaccessible swamp terrains.

The findings of this study carry direct operational implications for environmental regulation, public health planning, and disaster response across the Niger Delta and comparable petroleum-producing coastal regions. For environmental regulators such as NOSDRA and State Ministries of Environment, the demonstrated capacity of Sentinel-2 derived NDVI and water contamination indices to flag high-risk settlements with zero

false negatives means that satellite-AI screening can realistically substitute for, or triage, the slower manual Joint Investigation Visit process, shortening the interval between spill occurrence and intervention. For public health authorities, the strong statistical association between the Water Contamination Index and respiratory and dermatological morbidity (R^2 = 0.778 and 0.739, respectively) provides a quantifiable, spatially explicit basis for pre-positioning mobile clinics, potable water units, and epidemiological surveillance in creek-dependent communities before morbidity peaks are reached, rather than responding only after clinical caseloads rise. For oil-sector regulators and operating companies, the use of NDVI recovery trajectories as an objective, remotely verifiable benchmark offers a mechanism to hold remediation efforts accountable in terrain that is otherwise difficult and hazardous to inspect on foot. Collectively, these implications support a shift from reactive, field-report-driven governance toward a proactive, data-driven surveillance paradigm that links ecological indicators directly to anticipated human health burden.

Prior remote-sensing investigations in the Niger Delta have predominantly addressed either ecological degradation or public health outcomes in isolation. Studies such as O'Farrell et al. (2025) and Jonathan et al. (2025) applied Earth observation and machine learning to quantify mangrove loss and canopy stress following oil spills, while Kuta et al. (2025) and Wekpe & Idisi (2024) used Sentinel and Google Earth Engine-derived vegetation indices to track long-term vegetation impacts; none of these efforts incorporated community morbidity data into a unified predictive framework. Conversely, epidemiological studies such as Oyeyemi et al. (2024), Oghenetega et al. (2022), and Gbadamosi & Aldstadt (2025) established associations between oil exposure and adverse health outcomes using cohort or survey-based designs, without leveraging satellite-derived environmental indicators at scale. SAR-based spill-detection studies (Li et al., 2023; Oseni et al., 2026; Dong et al., 2025) have achieved strong detection accuracy for the spills themselves but stop short of linking detections to downstream human health risk. The classification performance obtained here (95.56% accuracy; 100% recall for SVM) is consistent with, and in the case of recall exceeds, accuracy ranges typically reported for oil-spill and land-cover classification tasks in the Niger Delta literature (Talukdar et al., 2020; Yekeen & Balogun, 2020), while the NDVI degradation gradients observed (0.38–0.44 baseline falling to <0.18) closely mirror the severe mangrove dieback thresholds reported by Nababa et al. (2020) and Barenblitt et al. (2024). This study therefore corroborates the ecological severity reported in earlier remote-sensing work while extending it, for the first time in this geographic context, into a quantitative, morbidity-linked risk classification system.

The principal novelty of this work lies in its integration, within a single supervised-learning framework, of three data streams that earlier studies have treated separately: multi-temporal Copernicus Sentinel-2 multispectral Earth observation, a composite surface Water Contamination Index, and host-community clinical morbidity records, synthesized across 180 geographically distributed coastal incident settlements spanning 15 local government areas. Rather than detecting spills or vegetation stress as an end in itself, the framework is explicitly oriented toward predicting community health risk, benchmarking four distinct algorithm families (SVM-RBF, Random Forest, Gradient Boosting, and Logistic Regression) under a stratified 5-fold cross-validation scheme to establish both performance and stability (CV F1 standard deviations of ±0.0175–±0.0203). To the authors' knowledge, this is among the first studies to couple Sentinel-2-derived vegetation and water-quality proxies with empirical respiratory and dermatological morbidity rates for oil-host communities in the Niger Delta into an operational, reproducible classification pipeline, rather than a purely descriptive or correlational analysis. The resulting framework is positioned not as a research exercise alone but as a deployable decision-support tool that regulatory, health, and disaster-response agencies can apply directly to prioritize field intervention in a region where conventional surveillance infrastructure is sparse.

Several limitations should be considered when interpreting these findings. First, the dataset comprised 180 incident settlements, limiting subgroup analyses and generalizability beyond the Niger Delta. Second, reliance on secondary clinical and facility records may introduce reporting and measurement biases due to under-reporting, inconsistent diagnostic coding, and differences in healthcare-seeking behaviour. Third, Sentinel-2 NDVI retrievals are susceptible to cloud cover, atmospheric haze, and seasonal variation despite multi-temporal compositing, potentially affecting model performance. Fourth, the exclusive use of optical imagery excluded Synthetic Aperture Radar (SAR), which could improve monitoring under cloudy conditions. Fifth, the cross-sectional design identifies predictive associations but cannot establish causality between

environmental contamination and health outcomes. Also, external validation in other oil-producing deltaic regions is required to assess model generalizability.

Sixth, the 1.9:1 class imbalance between high-risk and low-risk settlements, together with spatial autocorrelation among settlements within the same local government area, inflates standard stratified cross-validation performance relative to the spatially blocked results reported in Section 3.4; the spatially blocked F1-scores, while still indicative of useful predictive skill, represent a more conservative and realistic estimate of out-of-area generalizability. Seventh, because the Water Contamination Index and environmental extrapolation procedure described in Section 2.3 were used to extend the original NOSDRA incident log to 180 settlements, performance estimates are partly dependent on the validity of that extrapolation and should be revisited as additional field-verified records become available.

5. CONCLUSIONS

This study successfully developed and validated an integrated artificial intelligence and satellite Earth observation framework for monitoring crude-oil environmental degradation and predicting community health hazards in coastal Nigeria. By harmonizing Copernicus Sentinel-2 multispectral imagery, surface water contamination measurements, and host community morbidity records across 180 incident locations, our models demonstrated exceptional diagnostic power. The Support Vector Machine classifier achieved 95.56% overall accuracy and 100% sensitivity in isolating high-risk health settings, while multi-temporal satellite analysis tracked severe mangrove canopy defoliation and persistent ecological stress.

Based on these results, we recommend the following strategic actions: (i) regulatory deployment: the National Oil Spill Detection and Response Agency (NOSDRA) and State Ministries of Environment should integrate automated Sentinel-2 multispectral ingestion and SVM classification pipelines into the National Oil Spill Monitor to enable near-real-time disaster detection and automated damage severity scoring; (ii) targeted public health infrastructure: Ministries of Health must utilize AI risk maps to deploy targeted medical resources, clean potable drinking water filtration units, and mobile clinics to remote riverine communities situated within severe contamination corridors (WCI > 0.75); and (iii) mandatory ecosystem restoration: Oil operating companies should be held to strict restoration timelines utilizing satellite NDVI metrics as legally verifiable benchmarks of ecological recovery before cleanup certification is granted.

DECLARATIONS

Author Contributions

Olutomisin M. Orogbemi: Conceptualization, Methodology, Software, Data curation, Formal analysis, Investigation, Visualization, Writing original manuscript. Adeyemi M. Oduwole: Validation, Resources, review and editing. Adebayo O. Adetunmbi: Conceptualization, Supervision, Project administration, review and editing. All authors have read, critically revised, and approved the final version of the manuscript and agree to be accountable for all aspects of the work.

Funding

This research received Institutional-Base Research (IBR) Grant from the Tertiary Education Trust Fund (TETFund) through Olusegun Agagu University of Science and Technology, Okitipupa, Nigeria.

Conflict of Interest

The authors declare that they have no known competing financial interests or personal relationships that could have appeared to influence the work reported in this paper.

Data Availability Statement

The Sentinel- 2 Level -2A satellite imagery used in this study are freely available from the European Space

Agency's Copernicus Open Access Hub (https://scihub.copernicus.eu). The derived water contamination indices, geospatial incident coordinates, and de-identified community morbidity data supporting the findings of this study are available from the corresponding author upon reasonable request, subject to institutional and community data-sharing agreements.

Ethical Approval and Consent to Participate

This study relied on aggregated, de-identified secondary environmental and community-level health morbidity records; no individual patient-identifiable data were accessed or analyzed.

Consent for Publication

Not applicable, as this manuscript does not contain any individual person's identifiable data, images, or clinical details.

Acknowledgments

The authors gratefully acknowledge the European Space Agency (ESA) for open access to Copernicus Sentinel-2 imagery, and the regulatory and community health institutions that supported access to environmental incident and morbidity records used in this study

REFERENCES

1. Adebangbe, S. A., Dixon, D. P., & Barrett, B. (2025). Evaluating contaminated land and the environmental impact of oil spills in the Niger Delta region: A remote sensing-based approach. Environmental Monitoring and Assessment, 197, Article 1149. https://doi.org/10.1007/s10661-025-14584-4
2. Agumagu, O. O., Marchant, R., & Stringer, L. C. (2025). Land use and land cover change dynamics in the Niger Delta region of Nigeria from 1986 to 2024. Land, 14(4), Article 765. https://doi.org/10.3390/land14040765
3. Akinkpelumi, V. K., Ossai, C. M., Abdulai, P. M., Ozoani, H. A., Nwanaforo, E., Obasi, C. N., & Orisakwe, O. E. (2026). Human health risk assessment of metals and metalloid in food crops harvested from crude oil impacted community in Niger Delta, Nigeria. Scientific Reports, 16, Article 231. https://doi.org/10.1038/s41598-025-29676-x
4. Akinpelumi, V. K., Ezejiofor, A. N., Abdulai, P. M., Rovira, J., Frazzoli, C., & Orisakwe, O. E. (2025). Seasonal variations of physicochemical parameters, arsenic, heavy metals, and PAHs in groundwater and surface water in crude oil contaminated community of Niger Delta, Nigeria: A comparative chemometric and human health risk assessment analyses. Water Environment Research, 97(12), Article e70220. https://doi.org/10.1002/wer.70220
5. Akinwumiju, S. A., Adelodun, A. A., & Ogundeji, S. E. (2020). Geospatial assessment of oil spill pollution in the Niger Delta of Nigeria: An evidence-based evaluation of causes and potential remedies. Environmental Pollution, 267, Article 115545. https://doi.org/10.1016/j.envpol.2020.115545
6. Alotaibi, E., & Nassif, N. (2024). Artificial intelligence in environmental monitoring: In-depth analysis. Discover Artificial Intelligence, 4, Article 84. https://doi.org/10.1007/s44163-024-00198-1
7. Anucha, J. A., Kumar, S., Das, B., Nkwocha, I. L., Okpu, A., Patidar, S., Martínez-Villegas, N., & Sen Gupta, B. (2026). Multi-index satellite-based assessment of soil surface dynamics in the Niger Delta (Nigeria). Frontiers in Earth Science, 14, Article 1834748. https://doi.org/10.3389/feart.2026.1834748
8. Anyanwu, I. N., Beggel, S., Sikoki, F. D., Okuku, E. O., Unyimadu, J.-P., & Geist, J. (2023). Pollution of the Niger Delta with total petroleum hydrocarbons, heavy metals and nutrients in relation to seasonal dynamics. Scientific Reports, 13, Article 14079. https://doi.org/10.1038/s41598-023-40995-9
9. Barenblitt, A., Fatoyinbo, L., Thomas, N., Stovall, A., de Sousa, C., Nwobi, C., & Duncanson, L. (2024). Invasion in the Niger Delta: Remote sensing of mangrove conversion to invasive Nypa fruticans from 2015 to 2020. Remote Sensing in Ecology and Conservation, 10(1), 5–23. https://doi.org/10.1002/rse2.353

10. Binetti, M. S., Massarelli, C., & Uricchio, V. F. (2024). Machine learning in geosciences: A review of complex environmental monitoring applications. Machine Learning and Knowledge Extraction, 6(2), 1263–1280. https://doi.org/10.3390/make6020059
11. Chadalavada, S., Faust, O., Salvi, M., Seoni, S., Raj, N., Raghavendra, U., Gudigar, A., Barua, P. D., Molinari, F., & Acharya, R. (2025). Application of artificial intelligence in air pollution monitoring and forecasting: A systematic review. Environmental Modelling & Software, 185, Article 106312. https://doi.org/10.1016/j.envsoft.2024.106312
12. Cui, S., Gao, Y., Huang, Y., Shen, L., Zhao, Q., Pan, Y., & Zhuang, S. (2023). Advances and applications of machine learning and deep learning in environmental ecology and health. Environmental Pollution, 335, Article 122358. https://doi.org/10.1016/j.envpol.2023.122358
13. Dong, S., Feng, J., Gu, Z., Yin, K., & Long, Y. (2025). A review of artificial intelligence and remote sensing for marine oil spill detection, classification, and thickness estimation. Remote Sensing, 17(22), Article 3681. https://doi.org/10.3390/rs17223681
14. Ewim, D. R. E., Orikpete, O. F., Scott, T. O., Onyebuchi, C. N., Onukogu, A. O., Uzougbo, C. G., & Onunka, C. (2023). Survey of wastewater issues due to oil spills and pollution in the Niger Delta area of Nigeria: A secondary data analysis. Bulletin of the National Research Centre, 47, Article 116. https://doi.org/10.1186/s42269-023-01090-1
15. Gbadamosi, F., & Aldstadt, J. (2025). The interplay of oil exploitation, environmental degradation and health in the Niger Delta: A scoping review. Tropical Medicine & International Health, 30(5), 351–367. https://doi.org/10.1111/tmi.14108
16. Gryech, I., Asaad, C., Ghogho, M., & Kobbane, A. (2024). Applications of machine learning and Internet of Things for outdoor air pollution monitoring and prediction: A systematic literature review. Engineering Applications of Artificial Intelligence, 137(Part B), Article 109182. https://doi.org/10.1016/j.engappai.2024.109182
17. Himeur, Y., Rimal, B., Tiwary, A., & Amira, A. (2022). Using artificial intelligence and data fusion for environmental monitoring: A review and future perspectives. Information Fusion, 86–87, 44–75. https://doi.org/10.1016/j.inffus.2022.06.003
18. Huang, X., Zhang, B., Perrie, W., Lu, Y., & Wang, C. (2022). A novel deep learning method for marine oil spill detection from satellite synthetic aperture radar imagery. Marine Pollution Bulletin, 179, Article 113666. https://doi.org/10.1016/j.marpolbul.2022.113666
19. Igibah, C. E., Ilaboya, I. R., Iyeke, S. D., Ufuah, E., & Agashua, O. L. (2024). Health effects of oil and waste pollutants on Delta Nigeria inhabitants' well being and its mitigation. Emergency Management Science and Technology, 4, Article e017. https://doi.org/10.48130/emst-0024-0015
20. Jonathan, E. L., Imoni, O., Chukwuemeka, P., & Eteh, D. R. (2025). Impact of oil spills on mangrove ecosystem degradation in the Niger Delta using remote sensing and machine learning. Journal of Geography and Cartography, 8(2), Article 11707. https://doi.org/10.24294/jgc11707
21. Kang, J., Yang, C., Yi, J., & Lee, Y. (2024). Detection of marine oil spill from PlanetScope images using CNN and Transformer models. Journal of Marine Science and Engineering, 12(11), Article 2095. https://doi.org/10.3390/jmse12112095
22. Kanu, C. T., & Iwunze, E. C. (2024). Link between oil pollution and adverse pregnancy outcomes in the Niger Delta region of Nigeria. Asian Journal of Medicine and Health, 22(5), 67–79. https://doi.org/10.9734/ajmah/2024/v22i51012
23. Kazanskiy, N., Khabibullin, R., Nikonorov, A., & Khonina, S. (2025). A comprehensive review of remote sensing and artificial intelligence integration: Advances, applications, and challenges. Sensors, 25(19), Article 5965. https://doi.org/10.3390/s25195965
24. Krejcar, O., & Namazi, H. (2026). AI in remote sensing and satellite image processing: A review. Environmental Earth Sciences, 85, Article 78. https://doi.org/10.1007/s12665-025-12798-w
25. Kuta, A. A., Grebby, S., & Boyd, D. S. (2025). Remote monitoring of the impact of oil spills on vegetation in the Niger Delta, Nigeria. Applied Sciences, 15(1), Article 338. https://doi.org/10.3390/app15010338
26. Li, C., Kim, D.-J., Park, S., Kim, J., & Song, J. (2023). A self-evolving deep learning algorithm for automatic oil spill detection in Sentinel-1 SAR images. Remote Sensing of Environment, 299, Article 113872. https://doi.org/10.1016/j.rse.2023.113872

27. Méndez, M., Merayo, M. G., & Núñez, M. (2023). Machine learning algorithms to forecast air quality: A survey. Artificial Intelligence Review, 56, 10031–10066. https://doi.org/10.1007/s10462-023-10424-4
28. Nababa, I. I., Symeonakis, E., Koukoulas, S., Higginbottom, T. P., Cavan, G., & Marsden, S. (2020). Land cover dynamics and mangrove degradation in the Niger Delta region. Remote Sensing, 12(21), Article 3619. https://doi.org/10.3390/rs12213619
29. O'Farrell, J., O'Fionnagáin, D., Babatunde, A. O., Geever, M., Codyre, P., Murphy, P. C., Spillane, C., & Golden, A. (2025). Quantifying the impact of crude oil spills on the mangrove ecosystem in the Niger Delta using AI and Earth observation. Remote Sensing, 17(3), Article 358. https://doi.org/10.3390/rs17030358
30. Oghenetega, O. B., Okunlola, M. A., Ana, G. R. E., Morhason-Bello, O., & Ojengbede, O. A. (2022). Exposure to oil pollution and maternal outcomes: The Niger Delta prospective cohort study. PLOS ONE, 17(3), Article e0263495. https://doi.org/10.1371/journal.pone.0263495
31. Olise, F. S. (2025). Bridging data gaps in Nigerian air pollution: Coverage, infrastructural challenges, and public health implications. Environmental Science and Pollution Research, 32, 23331–23350. https://doi.org/10.1007/s11356-025-36949-5
32. Olukaejire, S. J., Ifiora, C. C., Osaro, P. A., Osuji, L. C., & Hart, A. I. (2024). Petroleum exploration in the Niger Delta region and implications for the environment: A review. Journal of Energy Research and Reviews, 16(5), 19–29. https://doi.org/10.9734/jenrr/2024/v16i5350
33. Onyena, A. P., Folorunso, O. M., Nwanganga, N., Udom, G. J., Ekhator, O. C., Frazzoli, C., Ruggieri, F., Bocca, B., & Orisakwe, O. E. (2024). Engaging One Health in heavy metal pollution in some selected Nigerian Niger Delta cities: A systematic review of pervasiveness, bioaccumulation and subduing environmental health challenges. Biological Trace Element Research, 202(4), 1356–1389. https://doi.org/10.1007/s12011-023-03762-5
34. Orisakwe, O. E. (2021). Crude oil and public health issues in Niger Delta, Nigeria: Much ado about the inevitable. Environmental Research, 194, Article 110725. https://doi.org/10.1016/j.envres.2021.110725
35. Orogbemi, O. M. & Ewaregbemi, S. E. (2026a). Development of ilajeland degradation system in crude oil exploitation areas using satellite imagery and support vector machine model. International Journal of Research and Innovation in Applied Science, ISSN No.: 2454-6194. DOI:
36. https://doi.org/10.51584/IJRIAS.2026.11070088
37. Orogbemi, O. M. & Balogun, J. T. (2026b). A machine learning-based health issues detections system in crude oil exploitation host communities in Ondo State. International Journal of Scientific Research and Modern Technology, Vol 5 (7). DOI: https://doi.org/10.38124/ijsrmt.v5i7.1582
38. Oseni, R. D., Omosanya, K. O. L., Mosuro, G. O., Saka, H. O., Oludipe, V. D., & Oshomoji, A. (2026). Mapping persistent oil spill risk in the Niger Delta using Sentinel-1 SAR and environmental exposure indicators. Marine Pollution Bulletin, 229, Article 119674. https://doi.org/10.1016/j.marpolbul.2026.119674
39. Oyebamiji, A., Hoque, M. A., & Whitworth, M. (2025). Regional assessment of groundwater contamination risk from crude oil spillages in the Niger Delta: A novel application of the source-pathway-receptor model. Earth Systems and Environment, 9, 117–133. https://doi.org/10.1007/s41748-024-00416-x
40. Oyeyemi, A. W., Owonikoko, W. M., Okoro, T. D., Adagbonyi, O., & Ajeigbe, K. O. (2024). Water contamination: A culprit of serum heavy metals concentration, oxidative stress and health risk among residents of a Nigerian crude oil-producing community. Toxicology Reports, 12, 375–388. https://doi.org/10.1016/j.toxrep.2024.03.006
41. Paheding, S., Saleem, A., Siddiqui, M. F. H., Rawashdeh, N. A., Essa, A., & Reyes, A. A. (2024). Advancing horizons in remote sensing: A comprehensive survey of deep learning models and applications in image classification and beyond. Neural Computing and Applications, 36, 16727–16767. https://doi.org/10.1007/s00521-024-10165-7
42. Peng, Z., Zhang, B., Wang, D., Niu, X., Sun, J., Xu, H., Cao, J., & Shen, Z. (2024). Application of machine learning in atmospheric pollution research: A state-of-art review. Science of the Total Environment, 910, Article 168588. https://doi.org/10.1016/j.scitotenv.2023.168588

43. Sartono, A., Darmawan, M., Ramadhani, F., Ramdhan, M., Safitri, S., & Sutejo, B. (2025). Environmental monitoring of shallow marine waters using AI and remote sensing: A systematic literature review. Environmental Quality Management, 35(1), Article e70148. https://doi.org/10.1002/tqem.70148
44. Subramaniam, S., Raju, N., Ganesan, A., Rajavel, N., Chenniappan, M., Prakash, C., Pramanik, A., Basak, A. K., & Dixit, S. (2022). Artificial intelligence technologies for forecasting air pollution and human health: A narrative review. Sustainability, 14(16), Article 9951. https://doi.org/10.3390/su14169951
45. Talukdar, S., Singha, P., Mahato, S., Shahfahad, Pal, S., Liou, Y.-A., & Rahman, A. (2020). Land-use land-cover classification by machine learning classifiers for satellite observations: A review. Remote Sensing, 12(7), Article 1135. https://doi.org/10.3390/rs12071135
46. Trujillo-Acatitla, R., Tuxpan-Vargas, J., & Ovando-Vázquez, C. (2022). Oil spills: Detection and concentration estimation in satellite imagery, a machine learning approach. Marine Pollution Bulletin, 184, Article 114132. https://doi.org/10.1016/j.marpolbul.2022.114132
47. Tsiakos, C.-A. D., & Chalkias, C. (2023). Use of machine learning and remote sensing techniques for shoreline monitoring: A review of recent literature. Applied Sciences, 13(5), Article 3268. https://doi.org/10.3390/app13053268
48. Ukhurebor, K. E., Aigbe, U. O., Onyancha, R. B., Athar, H., Okundaye, B., Aidonojie, P. A., Siloko, B. E., Hossain, I., Kusuma, H. S., & Darmokoesoemo, H. (2024). Environmental influence of gas flaring: Perspective from the Niger Delta region of Nigeria. Geofluids, 2024, Article 1321022. https://doi.org/10.1155/2024/1321022
49. Wang, D., Dai, Z., Long, C., Liang, X., Xiong, Y., & Cheng, J. (2025). The serious loss of mangrove forest over the largest delta of Africa, Niger Delta: Causes and reasons. Marine Environmental Research, 210, Article 107350. https://doi.org/10.1016/j.marenvres.2025.107350
50. Wekpe, V. O., & Idisi, B. E. (2024). Long-term monitoring of oil spill impacted vegetation in the Niger Delta region of Nigeria: A Google Earth Engine derived vegetation indices approach. Journal of Geography, Environment and Earth Science International, 28(2), 27–40. https://doi.org/10.9734/jgeesi/2024/v28i2748
51. Yekeen, S. T., & Balogun, A.-L. (2020). Advances in remote sensing technology, machine learning and deep learning for marine oil spill detection, prediction and vulnerability assessment. Remote Sensing, 12(20), Article 3416. https://doi.org/10.3390/rs12203416
52. Yuan, Q., Shen, H., Li, T., Li, Z., Li, S., Jiang, Y., Xu, H., Tan, W., Yang, Q., Wang, J., Gao, J., & Zhang, L. (2020). Deep learning in environmental remote sensing: Achievements and challenges. Remote Sensing of Environment, 241, Article 111716. https://doi.org/10.1016/j.rse.2020.111716
53. Zhang, Z., Zhang, S., Chen, C., & Yuan, J. (2024). A systematic survey of air quality prediction based on deep learning. Alexandria Engineering Journal, 93, 128–141. https://doi.org/10.1016/j.aej.2024.03.031